

Non-collinear magnetoconductance of a quantum dot

Jonas N. Pedersen^{1,2}, Jesper Q. Thomassen¹, and Karsten Flensberg¹

Nano-Science Center, Niels Bohr Institute, Universitetsparken 5, 2100 Copenhagen, Denmark.

²Department of Physics, University of Lund, Box 118, 22100 Lund, Sweden.

(Dated: June 29, 2018)

We study theoretically the linear conductance of a quantum dot connected to ferromagnetic leads. The dot level is split due to a non-collinear magnetic field or intrinsic magnetization. The system is studied in the non-interacting approximation, where an exact solution is given, and, furthermore, with Coulomb correlations in the weak tunneling limit. For the non-interacting case, we find an anti-resonance for a particular direction of the applied field, non-collinear to the parallel magnetization directions of the leads. The anti-resonance is destroyed by the correlations, giving rise to an interaction induced enhancement of the conductance. The angular dependence of the conductance is thus distinctly different for the interacting and non-interacting cases when the magnetizations of the leads are parallel. However, for anti-parallel lead magnetizations the interactions do not alter the angle dependence significantly.

I. INTRODUCTION

Spin transport through hybrid structures of both semiconductor and metal systems is now a well-established field of research¹. In recent years, also spin transport through quantum dots formed by nanotubes, molecular systems or nanoparticles has started to attract attention both experimentally^{2,3,4,5,6,7,8} and theoretically.^{9,10,11,12,13,14,15,16} One of the motivations for this has been the possibility of using quantum dots with a single spin as qubits, but naturally also a number of fundamental questions arise on how the interplay of spin coherence and interactions influences the transport.

When the spin coherence is maintained during the electron passage through the mesoscopic structure, the transport needs to be described in a coherent fashion at least for spin degree of freedom. Even for weak tunneling one therefore has to modify the usual rate equation approach if the magnetization directions are non-collinear.^{9,13,14} For stronger tunneling coupling also many of the non-equilibrium Green's function methods fail to describe the case when both interactions and spin coherence are important, such as for example the Hubbard I approximations used in Refs. 15,16.¹⁹

For the strong coupling case, a particular interesting situation occurs when the mesoscopic system has a magnetization which is non-collinear with respect to that of the ferromagnetic leads, which is what is studied in this paper. We study the conductance of a single-level quantum dot connected to ferromagnetic leads, and, in addition, the spin states of the quantum dot being split due to, e.g., an applied magnetic field. Experimentally, one could realize this geometry if the magnetic leads are fabricated as magnetic thin films, where the magnetic field is strongly pinned in the plane parallel to the film, so that a small magnetic field component can be applied to the quantum dot without changing the magnetization direction of the leads. The geometry of the device is illustrated in Fig. 1. We describe the system using a modified Anderson Hamiltonian where the leads are assumed to be polarized and the magnetic field gives rise to an

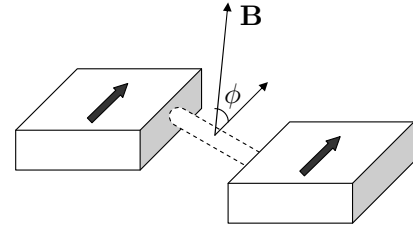


FIG. 1: Schematic drawing of the quantum dot system, connected to two ferromagnetic leads. In addition, there is an applied magnetic which spin polarizes the quantum dot in a direction non-collinear to the magnetization of the leads. In this paper, we focus on how the conductance depends on the angle ϕ , and the interplay between interactions and spin interference.

energy splitting of the dot level. This gives an effective double-slit geometry with two different paths through the central region. In the case of parallel magnetizations of the leads and no Coulomb repulsion on the dot, we find sharp anti-resonances in the conductance for certain angles ϕ , which is explained as destructive interference. If the Coulomb repulsion on the dot is increased, a cross-over to a simple spin-valve behavior is seen. Changing the angle ϕ in an experimental setup can therefore indicate whether interactions on the dot are important or if a single-electron picture is sufficient. On the other hand, in the case of anti-parallel magnetizations of the leads no change in the angular dependence is observed when the Coulomb repulsion on the dot is increased. Finally, we limit ourselves in this paper to the study of linear response, so non-equilibrium effects associated with spin accumulation are not included.

The paper is organized as follows. In Section II, we set up the model Hamiltonian. We start by calculating the conductance for the non-interacting case in Section III, and in Section IV we consider the cotunneling limit. Finally, in Section V we discuss the result and its limitations.

II. MODEL HAMILTONIAN

The model Hamiltonian of the quantum dot coupled to magnetic leads is

$$H = H_{LR} + H_T + H_D, \quad (1)$$

where

$$H_{LR} = \sum_{\alpha=L,R,k\sigma} \xi_{\alpha,k\sigma} c_{\alpha,k\sigma}^\dagger c_{\alpha,k\sigma}, \quad (2)$$

where α denotes the left or right electrode and where we have assumed that the polarizations of the electrodes are parallel or anti-parallel. The magnetization of the quantum dot is not necessarily parallel to those of the leads and in the spin basis of the leads, the dot Hamiltonian is

$$H_D = \sum_{\sigma} \xi_0 d_{\sigma}^\dagger d_{\sigma} + U n_{\uparrow} n_{\downarrow} + \sum_{\sigma\sigma'} \mathbf{B} \cdot \boldsymbol{\sigma}_{\sigma\sigma'} d_{\sigma}^\dagger d_{\sigma'}, \quad (3)$$

where ξ_0 is the orbital quantum dot energy, B represents the magnetic field splitting, and U is the Coulomb energy for double occupancy. In a diagonal basis, the dot Hamiltonian is

$$H_D = \sum_{\sigma} (\xi_0 + \sigma B) \tilde{d}_{\sigma}^\dagger \tilde{d}_{\sigma} + U \tilde{n}_{\uparrow} \tilde{n}_{\downarrow}, \quad (4)$$

where the d and \tilde{d} operators are related by the unitary rotation

$$d_{\sigma} = \sum_{\sigma'} R_{\sigma\sigma'} \tilde{d}_{\sigma'}, \quad \mathbf{R} = \begin{pmatrix} \cos(\phi/2) & \sin(\phi/2) \\ -\sin(\phi/2) & \cos(\phi/2) \end{pmatrix}. \quad (5)$$

Finally, the tunneling Hamiltonian is

$$H_T = \sum_{\alpha=L,R} \sum_{k\sigma\sigma'} \left(t_{\alpha,k\sigma} R_{\sigma\sigma'} c_{\alpha,k\sigma}^\dagger \tilde{d}_{\sigma'} + \text{h.c.} \right). \quad (6)$$

Here we allow for the tunneling matrix element to be spin dependent, because the states in the leads depend on spin direction. The possibility of spin flip processes during the tunneling process is not included explicitly here, however, it could easily be included by replacing the diagonal matrix t_{σ} by a non-diagonal tunneling matrix. Depending on parameters this would correspond to having an angle between the lead magnetizations, which would modify the details but not the general behaviors that we discuss.

III. RESONANT TUNNELING WITHOUT CORRELATIONS

We start by discussing the current through the system in absence of correlations, i.e. $U = 0$. This treatment is relevant where mean-field approaches are valid (of course

ξ_0 should be determined self-consistently), e.g. for a resonant tunneling junction system. The conductance follows from the Landauer formula as

$$G = \frac{e^2}{h} \int d\epsilon T(\epsilon) \left(-\frac{\partial n_F(\epsilon)}{\partial \epsilon} \right), \quad (7)$$

where $T(\epsilon)$ is the total transmission coefficient for both spin directions, and n_F is the Fermi-Dirac distribution function. In terms of the retarded and advanced Green's function the transmission coefficient is¹⁷

$$T(\epsilon) = \text{Tr} [\mathbf{G}^a(\epsilon) \mathbf{\Gamma}^R(\epsilon) \mathbf{G}^r(\epsilon) \mathbf{\Gamma}^L(\epsilon)], \quad (8)$$

with (using the spin basis where H_D is diagonal)

$$\mathbf{G}^{r,a}(\epsilon) = (\mathbf{G}_0^{-1} - \boldsymbol{\Sigma}_L^{r,a}(\epsilon) - \boldsymbol{\Sigma}_R^{r,a}(\epsilon))^{-1}, \quad (9a)$$

$$[\mathbf{G}_0(\epsilon)]_{\sigma\sigma'} = \delta_{\sigma,\sigma'} (\epsilon - \xi_0 - \sigma B)^{-1}, \quad (9b)$$

$$[\boldsymbol{\Sigma}_\alpha^{r,a}(\epsilon)]_{\sigma\sigma'} = \sum_{k\sigma''} (R^\dagger)_{\sigma\sigma''} |t_{\alpha,k\sigma''}|^2 g_{\alpha,k\sigma''}^{r,a}(\epsilon) R_{\sigma''\sigma'}, \quad (9c)$$

where $g_{\alpha,k\sigma}^{r,a}(\epsilon) = (\epsilon - \xi_{\alpha,k\sigma} \pm i0^+)^{-1}$ and $\mathbf{\Gamma}_\alpha = -i[\boldsymbol{\Sigma}_\alpha^r - \boldsymbol{\Sigma}_\alpha^a]$. In order to simplify the analysis, we assume that parts corresponding to the real parts of $g^{r,a}$ give constant shift of ξ_0 and hence can be incorporated in \mathbf{G}_0 , and, furthermore, that the tunnel width functions $\mathbf{\Gamma}_{L,R}$ are constant in energy. With these assumptions

$$\mathbf{\Gamma}_{L,R}(\epsilon) = \frac{\Gamma_{L,R}^0}{2} \begin{pmatrix} 1 + P_{L,R} \cos \phi & P_{L,R} \sin \phi \\ P_{L,R} \sin \phi & 1 - P_{L,R} \cos \phi \end{pmatrix}, \quad (10)$$

where

$$\Gamma_\alpha^0 = 2\pi \sum_{k\sigma} |t_{\alpha,k\sigma}|^2 \delta(\epsilon - \xi_{\alpha,k\sigma}) = \sum_{\sigma} \Gamma_{\alpha,\sigma}^0, \quad (11)$$

and P_α denotes the polarization of the tunneling from lead α defined through $\Gamma_{\alpha,\sigma}^0 = \frac{1}{2}(1 + \sigma P_\alpha) \Gamma_\alpha^0$. Finally, we have

$$\mathbf{G}^{r,a}(\epsilon) = ([\mathbf{G}_0^{r,a}(\epsilon)]^{-1} \pm i(\mathbf{\Gamma}_L + \mathbf{\Gamma}_R)/2)^{-1}. \quad (12)$$

With these formulae it is straightforward to find the transmission coefficient.

In the following, we study the current using the simplifying case of fully polarized leads, i.e. half-metallic contacts. For the parallel configuration, $P_L = P_R = 1$, we obtain for the transmission function

$$T_P(\epsilon) = \frac{\Gamma_L^0 \Gamma_R^0}{B^2} \frac{[x - \cos \phi]^2}{(1 - x^2)^2 + y^2(x - \cos \phi)^2}, \quad (13)$$

where

$$x = \frac{\epsilon - \xi_0}{B}, \quad y = \frac{\Gamma_L^0 + \Gamma_R^0}{2B} = \frac{\Gamma^0}{2B}. \quad (14)$$

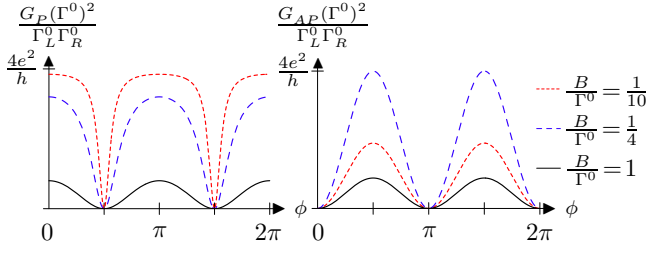


FIG. 2: (Colors online.) The conductance for the non-interacting case in both the parallel (left panel) and the antiparallel (right panel) cases for different values of the magnetic strength and at the symmetric point $\xi_0 = 0$. For the parallel case, destructive interference leads to an anti-resonance for $\phi = \pi/2$. The anti-resonance sharpens as B/Γ^0 decreases. The conductance is maximal when the applied field is parallel to magnetizations in the leads ($\phi = 0$ or π). In contrast, for the antiparallel case the current is maximal for $\phi = \pi/2$ and vanishes at $\phi = 0$ and π because of the spin-valve effect.

Let us look at the symmetric condition $x = 0$, where the incoming energy lies symmetrically between the spin split levels:

$$T_P(\xi_0) = \frac{\Gamma_L^0 \Gamma_R^0}{B^2} \frac{\cos^2 \phi}{1 + y^2 \cos^2 \phi}. \quad (15)$$

This yields a sharp anti-resonance when the dot magnetization is perpendicular to the magnetization direction of the leads. The anti-resonance occurs due to a destructive interference between the transmissions through the two spin split levels, as explained in the following section. It is interesting to note that the zero transmission at $\phi = \pi/2$ is not broadened by higher order tunneling events, as one might have expected. Moreover, for the non-symmetric situation $x \neq 0$, the anti-resonance remains, but is shifted away from $\phi = \pi/2$ to the point where $x = \cos \phi$, which follows from Eq. (13). The anti-resonance found here is in fact similar to an effect exploited in single atom transmission through optical lattices.¹⁸

Next, we look at the antiparallel situation. Therefore we set $P_L = -P_R = 1$ and find

$$T_{AP}(\epsilon) = \frac{4\Gamma_L^0 \Gamma_R^0}{B^2} \frac{\sin^2 \phi}{D}, \quad (16)$$

where

$$D = 4(1 - x^2)^2 + 2y_L y_R + y_L^2 y_R^2 / 4 + (y_R^2 + y_L^2)x^2 + 2(y_L^2 - y_R^2)x \cos \phi + (y_L - y_R)^2 \cos^2 \phi, \quad (17)$$

with $y_\alpha = \Gamma_\alpha^0 / B$. Note that for the symmetric coupling $\Gamma_L^0 = \Gamma_R^0$, the only angle dependence is the $\sin^2 \phi$ factor in the numerator. In Fig. 2 we show examples of the angle dependence of the conductance for both the parallel and antiparallel cases.

A difference between the parallel and antiparallel geometry is the existence of an optimal B -value in the antiparallel case. Considering the symmetric condition

$x = 0$, we find for the parallel case ($\phi = 0, \pi$)

$$T_P^{\max}(\xi_0) = \frac{\Gamma_L^0 \Gamma_R^0}{B^2 + (\Gamma^0/2)^2}, \quad (18)$$

which decreases when increasing B , because the levels are moved away from the chemical potentials of the leads. For the antiparallel geometry, the maximal transmission at the symmetric condition is ($\phi = \pi/2, 3\pi/2$)

$$T_{AP}^{\max}(\xi_0) = \frac{\Gamma_L^0 \Gamma_R^0}{[B + \Gamma_L^0 \Gamma_R^0 / (4B)]^2}, \quad (19)$$

and the optimal value $B_{\text{opt}} = \sqrt{\Gamma_L^0 \Gamma_R^0 / 4}$ is found. This value is a compromise between the spin blockade for $B = 0$ and the levels being far from the chemical potentials of the leads for $B/\Gamma^0 \gg 1$.

Finally, Fig. 3 shows how the conductance changes when ξ_0 is varied. In the parallel case, the destructive interference only occurs close to the symmetric condition, $x \approx 0$, whereas when both levels are above or below the resonance a simple spin valve effect is observed. If one of the levels is exactly at the chemical potentials of the leads the conductance is constant ($\xi_0 = \pm B$). For the antiparallel case no qualitative change in the angular dependence is seen.

IV. COTUNNELING CURRENT FOR THE INTERACTING CASE

In the presence of interactions the interesting interference effect discussed above can be significantly changed. Naturally, this is in general a difficult problem to tackle. Here we look at the case where the position of the levels is far from resonance as defined below, and a second order perturbation calculation suffices. This is the ‘‘cotunneling’’ regime, where an electron is transferred through the system in a two-electron process. The cotunneling approach is valid far from resonance, i.e. when $|\varepsilon_\uparrow - \mu|$ and $|\varepsilon_\downarrow + U|$ are larger than the bias, temperature and tunneling broadening.

For the resonant case the cotunneling result diverges and there is a cross-over to the sequential tunneling regime, see App. A. In these points interactions are not important, because transport is determined by only one level.

We calculate the current using a scattering formalism and the transition rate per unit time between an initial state i (with energy E_i) and a final state f (with energy E_f) is calculated as

$$\Gamma_{fi} = \frac{2\pi}{\hbar} |\langle f | T | i \rangle|^2 \delta(E_f - E_i), \quad (20)$$

where the transition operator \hat{T} is

$$\hat{T} = H_T + H_T \frac{1}{E_i - H_0 + i\eta} \hat{T} \quad (21)$$

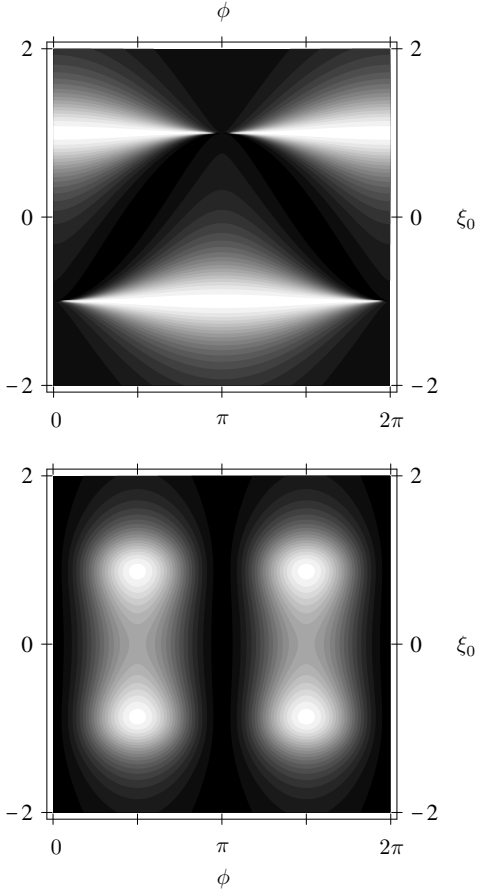


FIG. 3: Contour plots of the conductance in the non-interacting case for the parallel (top panel) and antiparallel (lower panel) geometry for different values of the angle ϕ and the orbital dot quantum dot energy ξ_0/Γ_0 ($B/\Gamma_0 = 1$ in both figures). For the antiparallel geometry the same angular dependence is observed for all ξ_0 , whereas a change is seen for the parallel geometry as explained in the text.

and $H_0 = H_{LR} + H_D$. The current is now given by processes which bring an electron from the left to the right lead, Γ_{RL} , minus the opposite processes:

$$J = e(\Gamma_{RL} - \Gamma_{LR}). \quad (22)$$

The transition rates will only be calculated to lowest non-vanishing order in the coupling. Thus, in the initial state the leads can be considered as two non-interacting electron gases (here assumed fully spin-polarized) with different chemical potentials. The probability to find the lead α in a state ν_α is denoted W_{ν_α} . Because the leads are non-interacting, W_{ν_α} satisfies

$$\sum_{\nu_\alpha} W_{\nu_\alpha} \langle \nu_\alpha | c_{\alpha,k\sigma}^\dagger c_{\alpha,k\sigma} | \nu_\alpha \rangle = n_F(\varepsilon_{\alpha,k\sigma} - \mu_\alpha). \quad (23)$$

Three different regimes are considered (see Fig. 4):

i) the level with the lowest energy is always occupied and the other energy level always empty, *i.e.* $\varepsilon_\uparrow < \mu$ and

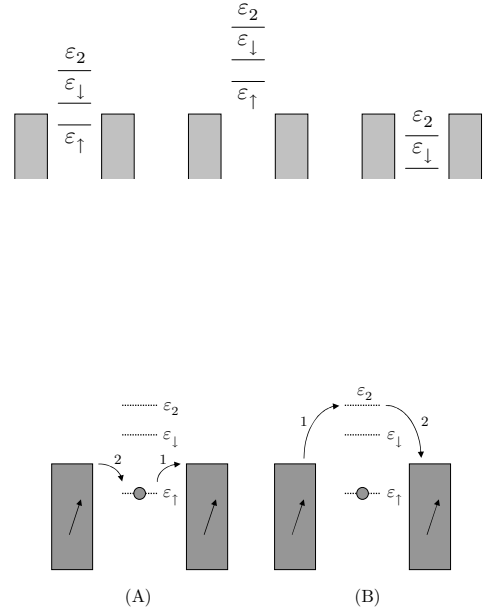


FIG. 5: The two possible second order processes contributing to the tunneling amplitude, here shown for the parallel configuration in the first regime. Because of interactions, the path to the right is suppressed when the lower energy spin-state is occupied by one electron. Hence the interactions tend to destroy the interference effects seen in Fig. 2, valid for $U = 0$, and instead one gets the angular dependence shown in Fig. 6.

$\varepsilon_\downarrow > \mu$,

ii) both levels are empty, *i.e.* $\varepsilon_\uparrow > \mu$ and $\varepsilon_\downarrow > \mu$,

iii) both levels occupied, *i.e.* $\varepsilon_\uparrow < \mu$ and $\varepsilon_\downarrow + U < \mu$.

We show how the result is obtained for the first regime with parallel geometry and only state the results for the other regimes.

In case *i*), the initial states can be written as $|i\rangle = |\nu_L, \nu_R, \uparrow\rangle$, with energy $E_i = E_{\nu_L} + E_{\nu_R} + \varepsilon_\uparrow$ and probability $W_{\nu_L} W_{\nu_R}$. First, we outline the derivation for Γ_{RL} in the parallel configuration. In the fully polarized case, the leads contain only electrons with one kind of spin, say spin-up, and the final states are $|f_{kk'}\rangle = c_{R,k\uparrow}^\dagger c_{L,k'\uparrow} |i\rangle$, meaning that an electron is moved from the left to the right lead in the process. Inserting the expressions for the final states and the tunneling Hamiltonian in Eqs. (20) and (21), we see that the first non-vanishing term is second order in the coupling H_T . Moreover, two processes give a contribution: A) first the electron on the dot jumps to the right lead and later an electron from the left lead refills the dot, or B) a left lead electron enters the dot, creating a double occupied state, and later leaves the dot to the right. The two processes are sketched in Fig. 5. The scattering rate $\Gamma_{RL}^{(i)}$ can now be written as

$$\Gamma_{RL}^{(i)} = \frac{2\pi}{\hbar} \sum_{kk'\nu_L\nu_R} W_{\nu_L} W_{\nu_R} |M_A + M_B|^2 \delta(\varepsilon_{R,k\uparrow} - \varepsilon_{L,k'\uparrow}), \quad (24)$$

where

$$M_A = \sum_{k_1 k_2} t_{L,k_2\uparrow}^* t_{R,k_1\uparrow} |R_{\uparrow,\uparrow}|^2 \quad (25)$$

$$\times \langle f_{kk'} | \tilde{d}_{\uparrow}^\dagger c_{L,k_2\uparrow} \frac{1}{E_i - H_0} c_{R,k_1\uparrow}^\dagger \tilde{d}_{\uparrow} | i \rangle, \quad (26)$$

$$M_B = \sum_{k_1 k_2} t_{L,k_2\uparrow}^* t_{R,k_1\uparrow} |R_{\downarrow,\uparrow}|^2$$

$$\times \langle f_{kk'} | c_{R,k_1\uparrow}^\dagger \tilde{d}_{\downarrow} \frac{1}{E_i - H_0} \tilde{d}_{\downarrow}^\dagger c_{L,k_2\uparrow} | i \rangle.$$

The matrix elements M_A and M_B are easily calculated, and after inserting the coupling constants in Eq. (11) and assuming them to be independent of energy, we arrive at

$$\Gamma_{RL}^{(i)} = \frac{\Gamma_L^0 \Gamma_R^0}{2\pi} \int d\epsilon \left[\frac{|R_{\uparrow,\uparrow}|^2}{\epsilon_{\uparrow} - \epsilon} - \frac{|R_{\downarrow,\uparrow}|^2}{\epsilon - \epsilon_{\downarrow} - U} \right]^2 \times n_F(\epsilon - \mu_L) [1 - n_F(\epsilon - \mu_R)]. \quad (27)$$

For $\Gamma_{LR}^{(i)}$ exactly the same calculations are carried out and we finally obtain for the current

$$J_P^{(i)} = \frac{e}{\hbar} \frac{\Gamma_L^0 \Gamma_R^0}{2\pi} \int d\epsilon \left[\frac{|R_{\uparrow,\uparrow}|^2}{\epsilon_{\uparrow} - \epsilon} - \frac{|R_{\downarrow,\uparrow}|^2}{\epsilon - \epsilon_{\downarrow} - U} \right]^2 \times [n_F(\epsilon - \mu_L) - n_F(\epsilon - \mu_R)]. \quad (28)$$

At small bias voltage, we use that $|\epsilon| \ll |\epsilon_{\uparrow}|, |\epsilon_{\downarrow} + U|$ and when inserting the form of \mathbf{R} from Eq. (5), we obtain

$$J_P^{(i)} = e^2 V \frac{\Gamma_L^0 \Gamma_R^0}{h} \left[\frac{\cos^2(\phi/2)}{\xi_0 - B} + \frac{\sin^2(\phi/2)}{\xi_0 + B + U} \right]^2, \quad (29)$$

where $\mu_L - \mu_R = eV$. Note that the two terms in the square brackets are the amplitudes for the two tunneling processes shown in Fig. 5. In Eq. (29) it is evident that a destructive interference between the two paths can occur at certain angles.

Of course, a similar calculations can be performed for the antiparallel configuration, and with the same constraints the result is

$$J_{AP}^{(i)} = e^2 V \frac{\Gamma_L^0 \Gamma_R^0}{4h} \left[\frac{1}{\xi_0 - B} - \frac{1}{\xi_0 + B + U} \right]^2 \sin^2 \phi. \quad (30)$$

Looking at this expression, it is clear that the constructive interference for the anti-parallel case is not sensitive to the angle, because both paths have the angular dependence.

The cotunneling results for regime *i*) are plotted in Fig. 6 for different values of the Coulomb repulsion U . It is easily verified that to second order in Γ and $U = 0$ the cotunneling results (29) and (30) and the exact results for $U = 0$ derived above coincide.

In the other two regimes similar calculations give

$$J_P^{(ii)} = e^2 V \frac{\Gamma_L^0 \Gamma_R^0}{h} \left[\frac{\cos^2(\phi/2)}{\xi_0 - B} + \frac{\sin^2(\phi/2)}{\xi_0 + B} \right]^2, \quad (31)$$

$$J_{AP}^{(ii)} = e^2 V \frac{\Gamma_L^0 \Gamma_R^0}{4h} \left[\frac{1}{\xi_0 + B} - \frac{1}{\xi_0 - B} \right]^2 \sin^2 \phi \quad (32)$$

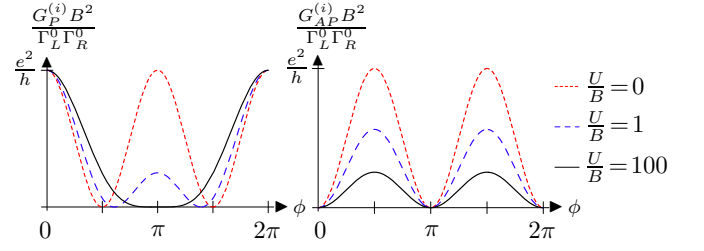


FIG. 6: (Colors online) The conductance for the *interacting* case in both the parallel (left panel) and the anti-parallel (right panel) cases for different values of the Coulomb interaction and for the symmetric point $\xi_0 = 0$. For the parallel case, we see how the anti-resonance at $\phi = \pi/2$ is destroyed by interactions, due to the blocking of one of the paths in Fig. 5. For large U one instead has a cross-over to a spin-valve effect at $\phi = \pi$, where the dot is occupied by an electron with spin opposite to the lead electrons. The angle dependence thus dramatically depends on the interaction. This is not so for the anti-parallel case shown in the right panel, where merely an overall suppressing is seen.

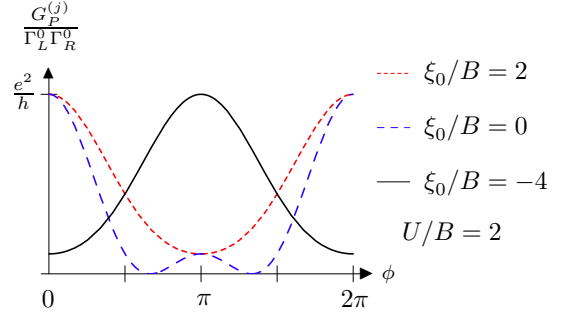


FIG. 7: (Colors online.) The cotunneling result for the parallel geometry in the three different regimes [$j = i, ii, iii$] with *i*) $\xi_0 = 0$, *ii*) $\xi_0/B = 2$ and *iii*) $\xi_0/B = -4$.

for both levels being empty, and

$$J_P^{(iii)} = e^2 V \frac{\Gamma_L^0 \Gamma_R^0}{h} \left[\frac{\cos^2(\phi/2)}{\xi_0 - B + U} + \frac{\sin^2(\phi/2)}{\xi_0 + B + U} \right]^2, \quad (33)$$

$$J_{AP}^{(iii)} = e^2 V \frac{\Gamma_L^0 \Gamma_R^0}{4h} \left[\frac{\sin \phi}{\xi_0 + B + U} - \frac{\sin \phi}{\xi_0 - B + U} \right]^2, \quad (34)$$

for both levels being occupied. Note that for $U = 0$ holds $J^{(i)} = J^{(ii)} = J^{(iii)}$, and it agrees with the non-interacting results in Sec. III to lowest order in $\Gamma_L^0 \Gamma_R^0$.

For the antiparallel geometry the same angular dependence is found for all three regimes with $G_{AP}^{(j)} \propto \sin^2 \phi$. Fig. 7 shows the conductance for the parallel geometry for the three different regimes. It is seen how the destructive interference only occurs in regime *i*), i.e. when the levels are split on each side of the chemical potentials and the interactions are not too strong. The angular dependence for the two other regimes depends on which level is closest to the chemical potential of the leads.

V. DISCUSSION AND SUMMARY

For the non-interacting case we found the exact linear response conductance. For the parallel configuration we saw that the angular dependence could be understood in terms of an interference effect occurring due to the spin-splitting of the dot. For $\phi = 0$ the spin bases of the dot and the leads are identical, and the electrons can only pass through the dot via the spin- \uparrow level. For a non-collinear magnetic field the dot spin eigenstates are superpositions of the lead spin states, which gives two possible paths through the dot. This leads to destructive interference at $\phi = \pi/2$, and the resonance sharpens as the tunneling coupling increases. This result is in agreement with the cotunneling result in Eq. (29) setting $U = 0$. Interestingly, the destructive interference is destroyed by interactions, giving rise to an interaction induced enhancement of the conductance. Thus the conductance goes from being proportional to $\cos^2 \phi$ in the non-interacting case to being proportional to $\cos^4(\phi/2)$ for the strongly interacting case. However, if the leads are not fully polarized the angular dependence persists, but is gradually washed out for decreasing polarization.

For the antiparallel geometry the situation is very different. In the non-interacting case (and symmetric coupling) the conductance is proportional to $\sin^2 \phi$ for all values of B/Γ^0 . This is simply understood as a spin-valve effect, giving zero conductance at $\phi = 0$ and $\phi = \pi$, whereas for non-collinear B -field the spin can flip when it passes the dot. Furthermore, in this case there is a constructive interference at $\phi = \pi/2$. Now, with interactions on the dot one spin channel becomes partially blocked, but the angular dependence remains the same even in the limit of large U . This is thus in stark contrast to the above mentioned cross-over observed for the parallel configuration.

We have thus focused on two cases: 1) strong tunneling and no interaction, and 2) weak tunneling with interaction. The cross-over between these two regimes is an interesting and challenging issue, because a formalism that captures both coherence and correlations on equal footing is needed.

APPENDIX A: SEQUENTIAL TUNNELING LIMIT FOR PARALLEL MAGNETIZATION

In the main part, we have discussed the effects of higher order tunneling where interference effects take place. For

completeness, we here give the results for the sequential tunneling limit for parallel magnetization.

In the parallel case, we can use the conductance formula derived by Meir and Wingreen¹⁷ for proportional coupling if we also assume that $P = P_L = P_R$. With these assumptions, we have

$$G = \frac{ie^2}{h} \int d\omega \left(-\frac{dn_F(\omega)}{d\omega} \right) \text{Tr} [\Gamma (\mathbf{G}^R(\omega) - \mathbf{G}^A(\omega))]. \quad (\text{A1})$$

where

$$\Gamma = \frac{\Gamma_L^0 \Gamma_R^0}{\Gamma_L^0 + \Gamma_R^0} \begin{pmatrix} 1 + P \cos \phi & P \sin \phi \\ P \sin \phi & 1 - P \cos \phi \end{pmatrix}.$$

To lowest order in the tunneling, which is the so-called sequential tunneling case, the Green's functions in Eq. (A1) are given by

$$i(\mathbf{G}^R - \mathbf{G}^A) = \begin{pmatrix} n_{\downarrow} \delta_{\uparrow}^U + (1 - n_{\downarrow}) \delta_{\uparrow}^0 & 0 \\ 0 & n_{\uparrow} \delta_{\downarrow}^U + (1 - n_{\uparrow}) \delta_{\downarrow}^0 \end{pmatrix}, \quad (\text{A2})$$

where

$$\delta_{\sigma}^A = 2\pi \delta(\omega - \varepsilon_{\sigma} - A), \quad (\text{A3})$$

and

$$n_{\uparrow, \downarrow} = \frac{e^{-\beta(2\xi_0 + U)} + e^{-\beta(\xi_0 \pm B)}}{1 + e^{-\beta(2\xi_0 + U)} + 2 \cosh(\beta B) e^{-\beta \xi_0}}, \quad (\text{A4})$$

where β is the inverse temperature. Thus for the parallel case, the conductance becomes a sum of four peaks:

$$\begin{aligned} \frac{G}{h/e^2} \frac{\Gamma_0}{\Gamma_L^0 \Gamma_R^0} &= (h(\xi_0 + B) [1 - n_{\downarrow}] + h(\xi_0 + B + U) n_{\downarrow}) \\ &\times (1 + P \cos \phi) \\ &+ (h(\xi_0 - B) [1 - n_{\uparrow}] + h(\xi_0 - B + U) n_{\uparrow}) \\ &\times (1 - P \cos \phi), \end{aligned} \quad (\text{A5})$$

where $h(\omega) = \left(-\frac{dn_F(\omega)}{d\omega} \right)$. This agrees with the non-interacting result for $U = 0$ and $\Gamma^0 \rightarrow 0$.

For the antiparallel geometry it is more complicated to obtain a simple result because the current formula in this case contains the lesser Green's function.¹⁷ The full rate equation results have been given in Ref. 13.

¹ I. Zutic, J. Fabian, and S. Das Sarma, Rev. Mod. Phys. **76**, 323 (2004).

² K. Tsukagoshi, B. W. Alphenaar, and H. Ago, Nature **401**, 572 (1999).

³ D. Orgassa, G. J. Mankey, and H. Fujiwara, Nanotechnology **12**, 281 (2001).

⁴ X. Hoffer, C. Klinke, J.-M. Bonard, L. Gravier, and J.-E. Wegrowe, cond-mat/0303314.

⁵ B. Zhao, I. Mönch, T. Mühl, H. Vinzelberg, and C. M. Schneider, J. Appl. Phys. **91**, 7026 (2002). B. Zhao, I. Mönch, H. Vinzelberg, T. Mühl, and C. M. Schneider, Appl. Phys. Lett. **80**, 3144 (2002).

- ⁶ J.-R. Kim, H. M. So, J.-J. Kim, and J. Kim, Phys. Rev. B **66**, 233401 (2002).
- ⁷ J. R. Petta, S. K. Slater, and D. C. Ralph, Phys. Rev. Lett. **93**, 136601 (2004)
- ⁸ A. Jensen, J. R. Hauptmann, J. Nygård, and P. E. Lindelof, unpublished.
- ⁹ J. König and J. Martinek, Phys. Rev. Lett. **90**, 166602 (2003).
- ¹⁰ J. Martinek, Y. Utsumi, H. Imamura, J. Barna, S. Maekawa, J. König, and G. Schön, Phys. Rev. Lett. **91**, 127203 (2003).
- ¹¹ J. Martinek, M. Sindel, L. Borda, J. Barna, J. König, G. Schön, and J. von Delft, Phys. Rev. Lett. **91**, 247202 (2003).
- ¹² W. Rudzinski and J. Barnas, Phys. Rev. B **64**, 085318 (2001).
- ¹³ M. Braun, J. König, and J. Martinek, Phys. Rev. B **70**, 1953435 (2004).
- ¹⁴ S. Braig and P. Brouwer, cond-mat/0412592.
- ¹⁵ W. Rudzinski, J. Barnas, R. Swirkowicz, and M. Wilczynski, cond-mat/0409386
- ¹⁶ J. Fransson, cond-mat/0502288
- ¹⁷ Y. Meir and N.S. Wingreen, Phys. Rev. Lett. **68**, 2512 (1998)
- ¹⁸ A. Micheli, A. J. Daley, D. Jaksch, and P. Zoller, quant-ph/040602.
- ¹⁹ T. Novotný and K. Flensberg, unpublished.